541

ENERGY RELEASE SITES IN MAGNETIC FIELDS CONTAINING SINGLE OR MULTIPLE NULLS

K. GALSGAARD, R. V. REDDY * and G. J. RICKARD **
University of St. Andrews, The Mathematical Institute, St. Andrews, Fife, KY16 9SS, Scotland

(Received 5 December 1996; accepted 15 May 1997

Abstract. An ongoing debate is how magnetic energy is released in solar flares, which type of magnetic instabilities are responsible for triggering the energy release, and which magnetic topologies are most likely to host the instabilities. In this connection magnetic reconnection has been a general ingredient, with most of the previous work focussing on 2D reconnection. A natural extension to this is to investigate reconnection in 3D topologies, in particular the behaviour of magnetic nulls and the magnetic topology associated with them. This paper investigates the difference in dynamical behaviour of a numerical domain that either contains a double null-point pair connected by a separator or only a fraction of the separator defined by the null-points. The experiments show that nulls can either accumulate current individually, or act together to produce a singular current collapse along the separator. The implication of these results for the interpretation of coronal data is discussed.

1. Introduction

Observations of the solar magnetic field reveal a high degree of complexity. High-resolution magnetograms measuring the strength and orientation of the vertical component of the magnetic field at the photosphere give the impression that positive and negative magnetic polarity is randomly scattered over most of the solar surface. Significant deviations from this random pattern are seen in the vicinity of sunspots, where single polarity field is assembled in large and usually highly irregular patterns. X-ray observations (*Yohkoh*, NIXT) reveal a magnetic field structure in the corona that is dominated by luminous magnetic loop structures that connect different polarity regions on the photosphere.

A conclusion from the observations is that, at least above a given length scale, the topology/connectivity of magnetic field lines above the photosphere must be complex. In a topologically complex field, separatrix surfaces divide the volume into independent regions of field lines.

Field lines that are close neighbours, but on either side of a separatrix surface, have foot point locations on the domain boundary that can be separated by distances that are on the order of the domain size. Separatrix surfaces may be introduced by the presence of magnetic null-points. Null-points are locations in space where the magnetic field vanishes and their spatial structure allows field lines from topologically distinct regions to come arbitrarily close together. With several

* Permanent address: Indian Institute of Geomagnetism Colaba, Bombay 400005, India.
** Permanent address: The Meteorological Office, London Road, Bracknell, Berkshire, RG12 2SZ, U.K.

separatrix surfaces in the magnetic domain, it is likely that they cross each other, defining so-called 'separator field lines'. Such a line is a natural part of some types of double null-point systems, but is also reported to exist in field configurations without null-points in the physically interesting part of the domain (above the photosphere).

In particular, Démoulin *et al.* (1994) investigate the magnetic field topology of a particular flare event. They use multiple magnetic sources to produce a 3D magnetic field that at the assumed photosphere resembles the vertical magnetic field seen in the magnetogram at the flare time. The 3D magnetic field was then used to determine positions of separatrix surfaces and separator lines in the domain. They find that the Hα kernels (high-intensity regions in Hα associated with the flare process) are located on or close to the separator lines. A larger survey along the same lines was made by Démoulin, Hénoux, and Mandrini (1994). They analysed eight flares obtaining 3D magnetic fields using the same techniques. From this investigation they find that magnetic null-points are only present above the photosphere for a minor number of the flares investigated and that they are not located close to the positions of energy release. They conclude that magnetic null-points are not needed for the fast energy release in flares, but that quasi-separator lines (Priest and Démoulin, 1995) are the locations of strong current concentrations that are needed for heating the plasma and producing the observed Hα kernels. Given these static and model-based constraints on the magnetic topology of the potential energy release sites, the question then arises as to the role played by separator lines with and without magnetic null-points in the dynamical evolution of magnetic field structures. The main thrust of this paper is an attempt to answer this very question.

Many have seen magnetic null-points as locations where free magnetic energy can be released through magnetic reconnection (Green, 1989; Lau and Finn, 1990; Priest and Titov, 1995). In 2D, an x-type topology based on the presence of a magnetic null-point is the only location in space where it is possible to start magnetic reconnection. In 3D this is not the case, since the extra spatial freedom makes it possible to have magnetic reconnection occurring in domains where there are no magnetic null-points (Hesse and Schindler, 1988; Priest and Démoulin, 1995). Full understanding of magnetic reconnection in 3D is not achieved at present, though important ingredients for reconnection to occur are seen in different numerical experiments (Strauss, 1991; Otto, 1995; Galsgaard and Nordlund, 1996a, b, 1997; Dahlburg, Antiochos, and Norton, 1996). These experiments drive reconnection in different magnetic topologies, which makes it difficult to find a common topological factor useful for identifying potential reconnection regions in a magnetic field. The one common feature in these experiments is the presence of a stagnation flow centred on the region where magnetic reconnection takes place. The reason for this flow topology differs between the experiments. In some cases it is imposed directly by the boundary stressing, while for other experiments it arises naturally as the magnetic field responds to the evolving dynamics.

Analytical investigations of the possible ways that a single null-point can accommodate magnetic reconnection have been undertaken (Lau and Finn, 1990; Priest and Titov, 1995). The normal method is to use the kinematic approach, where the magnetic field line topology is taken to be time-independent and the mapping of responses of small boundary velocities are made for the full domain. At locations where the velocity maps into super-Alfvénic velocity the kinematic assumption fails. This is taken as an indication that non-ideal effects ('reconnection') have to occur to bring the velocity mapping down to sub-Alfvénic values. They find that the fan plane and the spine axis become spatial regions where reconnection is likely to evolve. Priest and Titov (1995) therefore proposed three distinct types of reconnection in three-dimensional configurations with null-points, namely *spine reconnection*, *fan reconnection* and *separator reconnection* with the current being concentrated on the spine, the fan and the separator, respectively. Rickard and Titov (1995) extended this work to a linear modal decomposition of the cold MHD equations around an axisymmetric single null-point in a cylindrical coordinate system. Each mode is labelled by the azimuthal mode number m. They find that there are only two linear modes capable of providing a current at the null-point, the $m = 0$ or the $m = 1$. Of these the $m = 1$ is identified as being the most likely to be triggered, providing a current accumulation in the fan plane and therefore being an example of fan reconnection. This is also found by Craig and Fabling (1996) in the only unique nonlinear analytical solution of the problem found at present.

The field-line topology of magnetic null-point pairs is more complicated, since, up to four magnetically independent regions are now produced. These are defined by the two null-point fan planes. If they intersect, they define a field line that connects the two null-points, the separator line. For this case the kinematic approach shows that, apart from the regions found for the single null-point, the separator line is also a potential site of magnetic reconnection. In a numerical experiment by Galsgaard and Nordlund (1997), where they stress a field that contains eight null-points, they find that current accumulates along the separator lines, and evolves into a current sheet where magnetic reconnection proceeds.

From an analytical standpoint, the simplest way to produce a separator field-line is to have a pair of nulls, hence our double null. However, this may be considered a leap of faith since we are not even sure as to the prevalence of single nulls in the solar corona, let alone double nulls. However, Lau (1993) has shown that double nulls are indeed feasible by consideration of the fields resulting from 'realistic' photospheric sources. Indeed Lau (1993) details exactly the locations of the nulls and their separator and uses the same kinematic arguments noted above to contend that currents will be expected on the separator itself. This gives us some confidence that our idealised equilibria have some relevance to the physical setting of the corona.

As has been noted, the topological structures of the spine curve and the fan plane play an important role in determining the nature of current accumulation in the vicinity of a magnetic null. This paper is going to extend this study by investigating the influence of the separator in null-point dynamics. Like the spine curve and the fan plane, the separator is an inherent topological feature, and clearly merits such a study. To that end the layout of the rest of the paper is as follows. The following section summarises single null-point topology and linear dynamics. Section three describes the numerical method, the magnetic configurations and stressing patterns used in the investigation. The fourth section discusses the results using double null-points as a starting condition, while section five concentrates on the separator line experiments. Finally, Section 6 provide the conclusions and their implications for the understanding of present flare theory in respect to Démoulin, Hénoux, and Mandrini (1994) and Priest and Démoulin (1995).

2. Single Null-Point Topology and Linear Dynamics

The topology of 3D single null-points has been discussed by several authors (Fukao *et al.*, 1975; Green, 1989; Lau and Finn, 1990; Galsgaard, 1991; Galsgaard and Nordlund, 1997; Priest and Titov, 1995; Parnell *et al.*, 1996). This section provides a short overview of the concepts that are important for the following discussion. As the paper deals with 3D null-point pairs, dynamical response to perturbations, the important findings for single null-points, as discussed by Rickard and Titov (1996), are outlined and later used as reference for the interpretation of the experiments in this paper.

In investigations of magnetic null-points, it is common to expand the field around the null-point in a first order Taylor series. In this approximation the magnetic field is given by

$$\mathbf{B}(\mathbf{r}) = \mathsf{M}\,(\mathbf{r} - \mathbf{r}_0)\,, \tag{1}$$

where $\mathbf{r}_0$ is the position of the null-point and M is the Jacobian 3×3 matrix of the magnetic field at $\mathbf{r}_0$. The magnetic field-line topology is characterised by the eigenvalues and their corresponding eigenvectors for the Jacobian matrix. The following description is restricted to the case where all three eigenvalues are real and non-zero. From the condition that the magnetic field is divergence free, $\nabla \cdot \mathbf{B} = 0$, it is seen that the sum of the three eigenvalues is zero. There are then two eigenvalues with the same sign and one, the numerically largest, of opposite sign. The eigenvectors related to the two numerically smallest eigenvalues (it can be assumed that they are positive without loss of generality) define a plane that the magnetic field lines do not penetrate (in the terminology of Priest and Titov (1996) the fan plane). The field lines in the fan plane start at the null-point and diverge away from this point. The form of the field lines depends on the relative orientation of the eigenvectors and the value of the eigenvalues. The last eigenvector defines an axis (the spine axis Priest and Titov (1995)) about which neighbouring field lines approach and eventually spread out over the fan plane. Only the field-line defining the axis reaches the plane and does so at the null-point. For a systematic

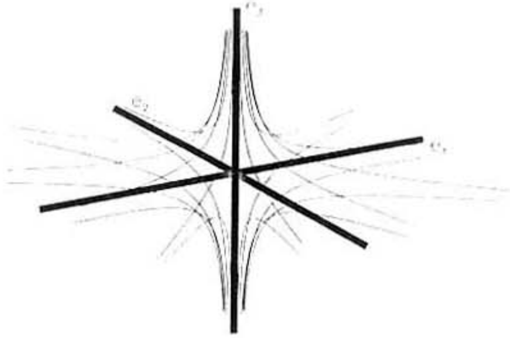

Figure 1. The field-line topology of a single null-point. e_1 and e_2 are the vectors that define the fan plane, and e_3 represents the direction of the spine axis.

description of the topological possibilities of magnetic null-points the reader is referred to Parnell *et al.* (1996). Figure 1 shows the field-line topology of an axisymmetric null-point (two equal eigenvalues and orthogonal eigenvectors).

Rickard and Titov (1996) have examined the dynamics of current accumulation around a single axisymmetric null-point using the cold linear MHD equations. The topology of the null-point makes it convenient to use cylindrical coordinates, where the z-axis represent the spine axis. They find that only the azimuthal modes $m = 0$ and $m = 1$ contribute to current at the null. The $m = 0$ is a pure Alfvénic wave mode and as such is confined to the field lines on which it is stimulated. This mode is driven by a vorticity flow centred on the spine axis, and focusses the perturbed magnetic energy along the spine axis. It is considered unimportant in comparison with the $m = 1$, which focusses the current at the null-point very efficiently. The $m = 1$ mode is triggered by either a systematic flow across the spine axis or by tilting the fan plane. In the first case the current direction through the null-point is orthogonal to the applied spine perturbation, while it in the second case is along the direction around which the fan plane is tilted. It is more likely that the coronal setting drives a $m = 1$ mode (i.e., fan reconnection) than a $m = 0$ (i.e., spine reconnection), as the centre of the flow and the spine axis have to be aligned before the $m = 0$ mode is triggered. We shall compare their results directly with the double null-point experiments in order to see which differences arise as a consequence of the modified field topology.

To our knowledge there have been no previous detailed nonlinear studies of the dynamical evolution of current structures at a three-dimensional null. Certainly others have shown that currents can be formed, but so far no real detail has been provided. The only nonlinear analysis to date is that of Craig *et al.* (1995), Craig and Henton (1995), and Craig and Fabling (1996), who provide exact steady-state reconnective solutions for three-dimensional nulls. The current structures they obtain are very reminiscent of those in Rickard and Titov (1996). Furthermore, the work of Craig and Fabling (1996) seems to agree with Rickard and Titov (1996) on the prime reconnective role of the $m = 1$ mode.

3. Numerical Methods – Experiments

The results in this paper are based on numerical investigations of the cold MHD equations, solving only the momentum and induction equation including both viscosity and resistivity:

$$\frac{\partial \mathbf{B}}{\partial t} = -\nabla \times \mathbf{E}\,, \tag{2}$$

$$\mathbf{E} = -(\mathbf{u} \times \mathbf{B}) + \eta \mathbf{j}\,, \tag{3}$$

$$\mathbf{j} = \nabla \times \mathbf{B}\,, \tag{4}$$

$$\frac{\partial \mathbf{u}}{\partial t} = \mathbf{j} \times \mathbf{B} + \nu \nabla^2 \mathbf{u} - (\mathbf{u} \times \nabla)\mathbf{u}\,, \tag{5}$$

where $\mathbf{u}, \mathbf{j}, \mathbf{B}, \nu$, and η are the flow velocity, the electric current, the magnetic field, the viscosity (constant) and the magnetic resistivity (constant), respectively. The equations are scaled such that $\mu_0 = 1$, and ρ is taken to be unity. They are solved using second-order differences to calculate space derivatives and a fourth-order Runge - Kutta - Gill method for the time advancing (Watanabe and Sato, 1990; Reddy *et al.*, 1995).

Boundary conditions are imposed on all domain sides, which are taken to be impenetrable and super-conducting. The footpoints of magnetic field lines are therefore frozen to the boundaries, and by applying velocities on these the magnetic field can be stressed. Predetermined velocity flows are imposed on a number of boundaries, while the velocity is kept zero on the remaining boundaries. These boundary conditions have the disadvantage that waves are reflected and reenter the domain. This typically happens after one Alfvén crossing time, after which both the magnetic field and the velocity field in the domain are somewhat influenced by it.

In deriving a 3D magnetic field structure from magnetograms, methods are used that assume that the magnetic field is either a potential or a force-free constant-α field. Démoulin, Hénoux, and Mandrini (1994) showed that both approximations are necessary to reach sufficiently good fits for all the magnetograms they investigated. This suggests that the two types of field may have a slightly different dynamical response to stress. We are therefore investigating both a potential and a force-free constant-α field with comparable field-line topology to quantify their dynamical behaviour. The magnetic fields are represented in a 3D Cartesian domain and the definitions contain magnetic null-points. The domain truncates the field to contain only the fraction of the field that is relevant for the given experiment. The two magnetic fields are defined as follows:

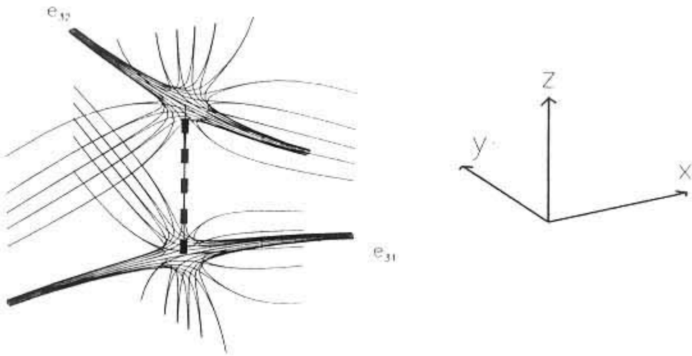

Figure 2. The field-line topology of the double null-point pair defined in Equation (6). The e_3s indicate the direction of the spine axes of the two null-points. The dotted line between the null-points outlines the location of the separator connecting the null-points. The nulls are located at the terminations of the dotted line. The local coordinate system is shown schematically on the right. The upper/lower spines are therefore aligned with the local y/x axes.

$$\mathbf{B}_p = \left(x(z-3), y(z+3), (1-z^2) + 0.5(x^2+y^2)\right) , \tag{6}$$

$$\mathbf{B}_{ff} = (\cos(2\pi y) - \sin(2\pi z), \cos(2\pi z) - \sin(2\pi x), \cos(2\pi x) - \sin(2\pi y)) \tag{7}$$

Equation (6) is a potential version of a magnetic field containing two null-points that was used by Priest and Titov (1996) in the kinematic investigation of double null-point separator reconnection. In the potential magnetic field case, Equation (6), the null-points are located at $(0, 0, \pm 1)$, with the respective spine axes in the $(1, 0, 0)$ and $(0, 1, 0)$ directions. The separator field-line is the part of the z-axis between the two null-points. The field in Equation (7) is the simplest force-free 3D periodic magnetic field that contains null-points. It in fact contains eight null-points per 3D period and was previously used by Galsgaard and Nordlund (1997) in their numerical study.

The double null-point topology can be understood from the topology of the single null-point. The null-points in a null-point pair can be orientated with respect to each other in a number of ways, with field lines connecting the null-points either along the spine axis or the fan plane (see, for example, the illustrations in Lau and Finn, 1990). The topology and relative orientation of the null-points investigated in this paper is that in which a single field line connects the null-points in their fan planes which is the structurally stable case (Priest and Titov, 1996). The fan plane from one null-point ends up along the spine axis of the other null-point, and *vice versa*. The field-line topology along the separator line is then, in a projection orthogonal to this line, like an x-point and the null-point pair divides space into four magnetically distinct regions in between them. Figure 2 gives an example of the field-line mapping around two magnetic null-points.

The force-free magnetic field, Equation (7), is 2π periodic in all three directions and contains as such eight null-points. We concentrate on a single null-point pair and have chosen the null-points at $(5, 5, 5)/8$ and $(3, 5, 7)/8$. The separator line lies in the (x, z)-plane and their spine axes are in the $(1, 1, 1)$ and $(1, -1, 1)$ directions, respectively. This null-point pair has the disadvantage that it is not aligned along any coordinate axis in the reference frame. To obtain a better orientation relative to the numerical domain, the coordinate system is both rotated and translated in a way that the separator line becomes aligned along the z-axis. The spine axes are then along $(\sqrt{\frac{2}{3}}, \sqrt{\frac{1}{3}}, 0)$ and $(\sqrt{\frac{2}{3}}, -\sqrt{\frac{1}{3}}, 0)$, respectively. The required transformations are given by

$$\mathbf{r} = \frac{1}{\sqrt{2}} \begin{pmatrix} 1 & 0 & -1 \\ 0 & \sqrt{2} & 0 \\ 1 & 0 & 1 \end{pmatrix} \mathbf{r}' + \frac{1}{8} \begin{pmatrix} 4 \\ 5 \\ 6 \end{pmatrix} , \tag{8}$$

$$\mathbf{B}' = \frac{1}{\sqrt{2}} \begin{pmatrix} 1 & 0 & 1 \\ 0 & \sqrt{2} & 0 \\ -1 & 0 & 1 \end{pmatrix} \mathbf{B} , \tag{9}$$

where the primed coordinates represent the numerical domain and the non-primed the domain in which the magnetic field, Equation (7), is defined. In some of the experiments a further rotation is made to align the spine axis of the null-point at $(3, 5, 7)/8$ along the x-direction.

We choose to stress our equilibrium fields by imposing motions on the boundary of the computational domain. This is intended to mimic the effect of photospheric footpoint motions in the solar corona. The choice of possible motions is clearly enormous. We therefore opt to examine those flows that we consider most likely to lead to interesting effects, in particular the generation of 'significant' currents. Experience dictates that we consider motions that cause the underlying magnetic topology to be altered, thereby forcing the field to attempt to readjust itself in order to return to a new equilibrium, usually via reconnection. As we shall see, vortex-type flows (that may exist) are eliminated on the grounds that they are unlikely to coincide with the features of the magnetic topology that would allow such flows to produce large currents. We therefore focus on the much more likely laminar flows, noting that they can always be decomposed into symmetric and antisymmetric components.

Applying super-conducting boundary conditions on all boundaries provides a limitation in the choice of the driving patterns that are easily applied. The patterns are restricted to those that join in a consistent way at the boundary edges. The easiest is to demand that the velocity goes to zero at the boundary edges. The prototype

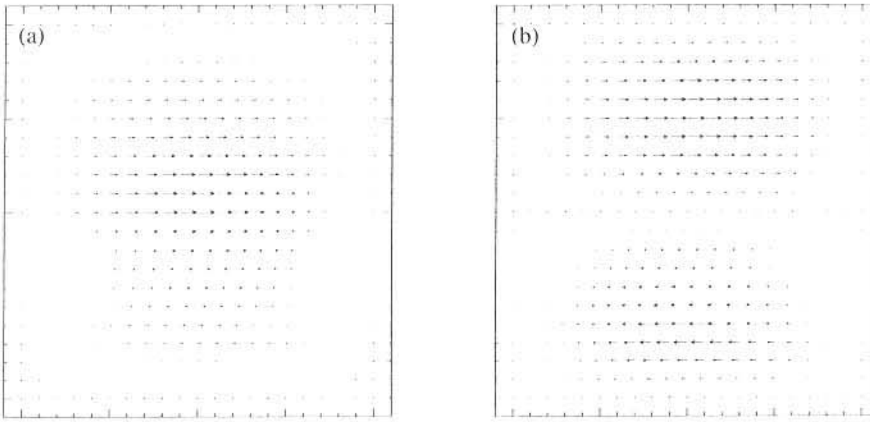

Figure 3. The topology of the two driving velocity profiles used. (a) The one-directional velocity (Equation (10)). (b) The shear velocity (Equation (11)).

of the two typical drives that are applied in this work represents a one-directional velocity and a shear velocity. These profiles are typically given by

$$\mathbf{u}_x(x, y, 0) = A_0(1 + \cos(\pi x))(1 + \cos(\pi y))/4\,, \tag{10}$$

$$\mathbf{u}_x(x, y, 0) = A_0(1 + \cos(\pi x))\sin(\pi y)/2\,, \tag{11}$$

where x and y are values in the interval $[-1, 1]$ and A_0 is the peak amplitude. The first gives a systematic velocity and the second a shear velocity profile (see Figure 3).

The basic equations represent the zero-β (gas pressure over magnetic pressure) limit, where magnetic forces provide the only contribution to the momentum equation. Effects arising from gas pressure gradients are not included in the investigation, even though neither of the drivers is incompressible and that this may prove to have an important influence on the dynamics close to the magnetic null-points, where the magnetic field by definition is weak. Comparisons with experiments using the full set of MHD equations show that, as long as A_0 is small compared to the Alfvén velocity and the maximum transport distance over the driving period is short compared to the domain size, the errors from not solving the continuity equation in the cold MHD experiments are not important for the final result.

Table I and Table II summarize the combinations of the driving profiles that are used for stressing the double null-point topologies. Table I contains the combinations applied on the z-boundaries (the separator line is along the z-direction). Table II shows the combinations applied on the x and y boundaries (the null-points spine axes penetrate the x and y boundaries). In Table I the type lower/upper indicate on which z-boundaries the driving pattern is applied. The A indicates a systematic velocity (velocity as in Equation (10)) across the fan plane and P a systematic velocity parallel to the fan plane. The $\pm$'s determine the direction of

Table I

Driving patterns on the plane orthogonal to the separator line (the z-boundaries). The type lower/upper represents the two boundaries. The P/A indicates systematic boundary driving (as in Equation (10)) parallel/across the fan plane. $\pm$ indicate the direction of the driving relative the relevant coordinate axis. Refer to Figure 2 for the local coordinate system.

No.	Type lower	Type upper
1	$P+$	$P+$
2	$P-$	$P+$
3	$A+$	$A+$
4	$A+$	$A-$
5	$A+$	$P+$
6	$A+$	$P-$

Table II

Driving patterns on one or more planes parallel to the separator line (the x-, y-boundaries). S is shear experiments with a velocity profile as in Equation (11). P is a systematic driving (as in Equation (10)) parallel to the separator line. O is a systematic driving (as in Equation (10)) orthogonal to the separator line. 25, 45, 75 represent systematic shear driving (as in Equation (10)) with the number giving the rotation angle relative to the P experiment. The numbers $(1, \frac{1}{2})$ describe on how large a fraction of the z boundary the driving is applied. When only $\frac{1}{2}$ of the boundary is perturbed, the driving velocity is always confined to the half where a spine axis is penetrating the surface. Refer to Figure 2 for the local coordinate system.

No.	x boundary	y boundary
1	$S\ \frac{1}{2}$	
2	$S\ \frac{1}{2}$	S $\frac{1}{2}$
3	S 1	
4		S 1
5	S 1	S 1
6	$P\ \frac{1}{2}$	
7	$O\ \frac{1}{2}$	
8	25 $\frac{1}{2}$	
9	45 $\frac{1}{2}$	
10	75 $\frac{1}{2}$	

the driving relative to the positive direction on the respective coordinate axis. For Table I x, y give the boundaries on which the driving is applied. S represents shear motion (as in Equation (11)) with the velocity being along the separator line (z-direction) and P/O represents systematic driving velocities parallel/orthogonal to the separator line (as in Equation (10)). The same type of driving is applied on both the upper and lower boundaries in the given coordinate direction. The amplitudes on two opposite boundaries are chosen to have different signs, thereby providing the largest shear between positions on the two boundaries. The numbers $(\frac{1}{2}, 1)$ appended after $S/P/O$ indicate the fraction of the boundary in the z direction that is involved in the driving. When this value is $\frac{1}{2}$, the driving is centred on the half part of the boundary where a spine axis penetrates the surface. In experiment 8–10 the numbers (25, 45, 75) give the direction of the driving relative to the separator line (see Figure 6). When velocities are applied on four boundaries and overlap in the z direction they are chosen such that the gradient of the velocity is continuous at the corners of the domain.

4. Double Null-Points

Very locally, the null-points in a null-point pair look like a single null-point, and all the knowledge from the single null-points may be used in understanding the behaviour of double null-points. In addition to this, a double null-point configuration contains a separator line. Both field configurations, Equation (6) and Equation (7), are initially force free. The force balance along the separator line arises as an equipartition between the field-line tension away from the line and the magnetic pressure towards the line. The projection of the field in a plane orthogonal to the separator line is initially an orthogonal x-point type. In 2D this structure is unstable, and as soon as the x-structure is perturbed, the magnetic tension force and magnetic pressure force will drive the x-point into a collapse and eventually form a current sheet (Syrovatskii, 1981). This may only be stopped if boundary conditions freeze the position of the foot points, and then this provides a balancing force that makes the collapse stop at a given angle. Close to the separator line in 3D, the same analysis becomes valid, so that the field may be separated into one component along the separator and two components in the plane perpendicular to this direction. The component along the separator provides a pressure in the plane and only weakly influences the actual dynamics that are driven by the imbalance between the tension and the magnetic pressure component in the plane. Then when field lines connecting to this region are perturbed by the boundary motion, an initial collapse of the region will occur until external forces stop the process.

This section gives a presentation of the experiments made with the magnetic fields defined in Equation (6) and Equation (7). The discussion is divided into two main sections, the first discusses results from the $m = \{0, 1\}$ mode experiments, while the second focusses on the shear stressing experiments.

4.1. $m = \{0, 1\}$ MODE PERTURBATIONS

The linear analysis by Rickard and Titov (1996) shows that a current accumulation at a single axisymmetric null-point is possible only for the azimuthal modes $m = \{0, 1\}$. The linear structure of the null-points, in both the potential and force-free magnetic fields defined above, has the same axisymmetric structure locally, but nonlinear effects already become important at a distance that is short compared to the null-point separation. Applying m mode perturbations to double null-point structures then provides us with information on the influence of the nonlinear field topologies on the dynamic evolution of the m modes.

There are two ways to drive the ($m = 0, 1$) modes in a single axisymmetric null-point: either by perturbing the field around the fan plane, or around the spine axis by applying velocities on the appropriate boundaries. The $m = 0$ mode is triggered by rotating the field lines around the spine axis. This may be done on either of the two boundaries, but it requires a good alignment of the perturbation with the magnetic null-point and spine axis. The $m = 1$ mode is much easier to initiate, requiring a tilt of the spine axis relative to the fan plane. This can be achieved either by a systematic flow (as in Equation (10)) across the spine axis or by tilting the fan plane by systematic velocities across the fan plane. The clean m modes are achieved only when preformed in a cylindrical coordinate system, but the same effects are obtained when the experiments are repeated with the null-point centred in a Cartesian box. In this case the two modes are most purely excited when perturbing the spine axis, though only minor differences are seen when they are excited by perturbations of the fan plane. To drive the m modes correctly by perturbing the fan plane, driving should be applied all the way around the null-point spine axis. This is not possible with two magnetic null-points in the numerical domain. Experiments with a single null-point in a Cartesian box show that the characteristic features of the m modes are still seen in the current accumulation when the fan plane is only perturbed on one of the four boundaries. A comparison between the current pattern of the four-sided and one-sided boundary driving of the $m = 1$ mode is illustrated in Figure 4 (a systematic velocity across the fan plane, as in Equation (10)). Despite the differences between the four-sided and one-sided driving, the same names are used here to characterise the double null-point experiments. This type of $m = 1$ experiments is represented by the entries in Table I, while a number of spine axis perturbations of the $m = 1$ mode are given by the experiment 6–10 in Table II.

4.1.1. *Potential Magnetic Field*

When the double null-point structure is perturbed by systematic velocities (Equation (10)) on the z-boundaries (the boundaries having the separator as a normal vector), the individual null-points are perturbed by one-sided fan perturbations (Table I). The experiments show that these one-sided m mode experiments behave similar to an isolated null-point. Figure 5 gives an impression of the current concentrations for the two m modes by showing isosurfaces of constant current strength and current vectors above a given threshold. The top panel shows the effect of the $m = 0$ perturbations on both z-boundaries (No. 1 of Table I), which clearly drives a current along the spine axis. The bottom panel represents two $m = 1$ mode perturbations (No. 3 of Table I) with the current accumulating in the fan planes. The conclusion from the experiments listed in Table I, is that the m modes driven from the z-boundaries do not generate current structures that are not already seen in the corresponding single null-point experiments.

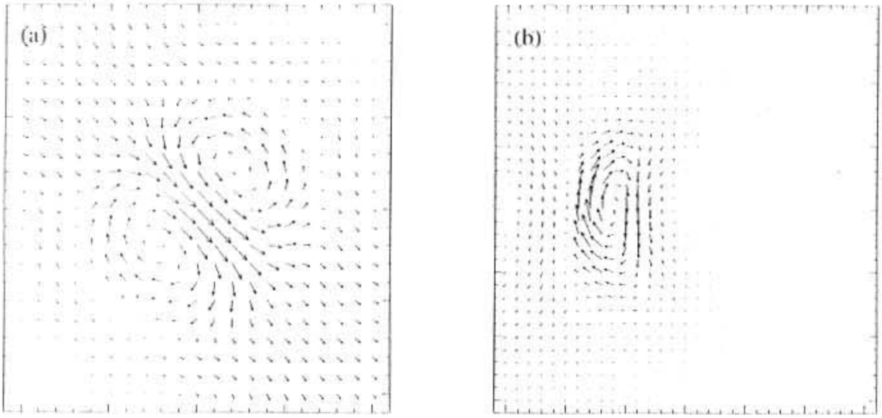

Figure 4. Current structures for $m = 1$ experiments shown for the fan plane of a single symmetric null-point. The $m = 1$ mode is driven here by applying velocities on the boundaries that are perpendicular to the plane shown and arranged in such a way that the fan plane is tilted around the direction of the current that runs through the null-point. (a) shows the case where driving is applied on all four sides of the domain. (b) gives the structure when the driving is applied only on one boundary (the left one).

When driving the $m = 1$ mode by perturbing the spine axis of a single null-point, the current accumulating at the null's fan plane has a direction through the null that is orthogonal to the imposed perturbation of the spine axis. This orthogonal relation between the orientation of the driving velocity and the generated current at the null-point is not in general valid for the same type of perturbation of one null in a pair. For this magnetic field topology the current is only orthogonal to the perturbing velocity when the driving is either parallel (No. 6 in Table II) or orthogonal (No. 7 in Table II) to the separator line. For any intermediate orientation of the driving (Nos. 8–10 in Table II), the part of the current profile that would be closest to the separator aligns itself with the separator line to a high degree. This is schematically shown in Figure 6, which shows the result of a velocity profile with a 45 degree rotation around the spine axis, relative to the direction of the separator line and the appearing current profile. The fraction of the current that aligns with the separator line depends on the orientation of the driving relative to the separator line. The larger the angle of deviation of the driving is from the ideal current alignment with the separator, the weaker the accumulating current magnitude becomes, although it is still clearly recognisable for angles on the order of 70 deg. As the angle increases, a third component starts to increase in strength, and it becomes the 'missing' half of the current as the rotation of the velocity profile reaches a 90-deg change. In the part of the fan plane that faces away from the separator line the current direction maintains its orientation relative to the driving profile. This is a clear example of the nonlinear magnetic field topology's influence on the current structure, visualising the separator line as a guiding devise that efficiently focusses the $m = 1$ mode perturbations of the spine axis to align

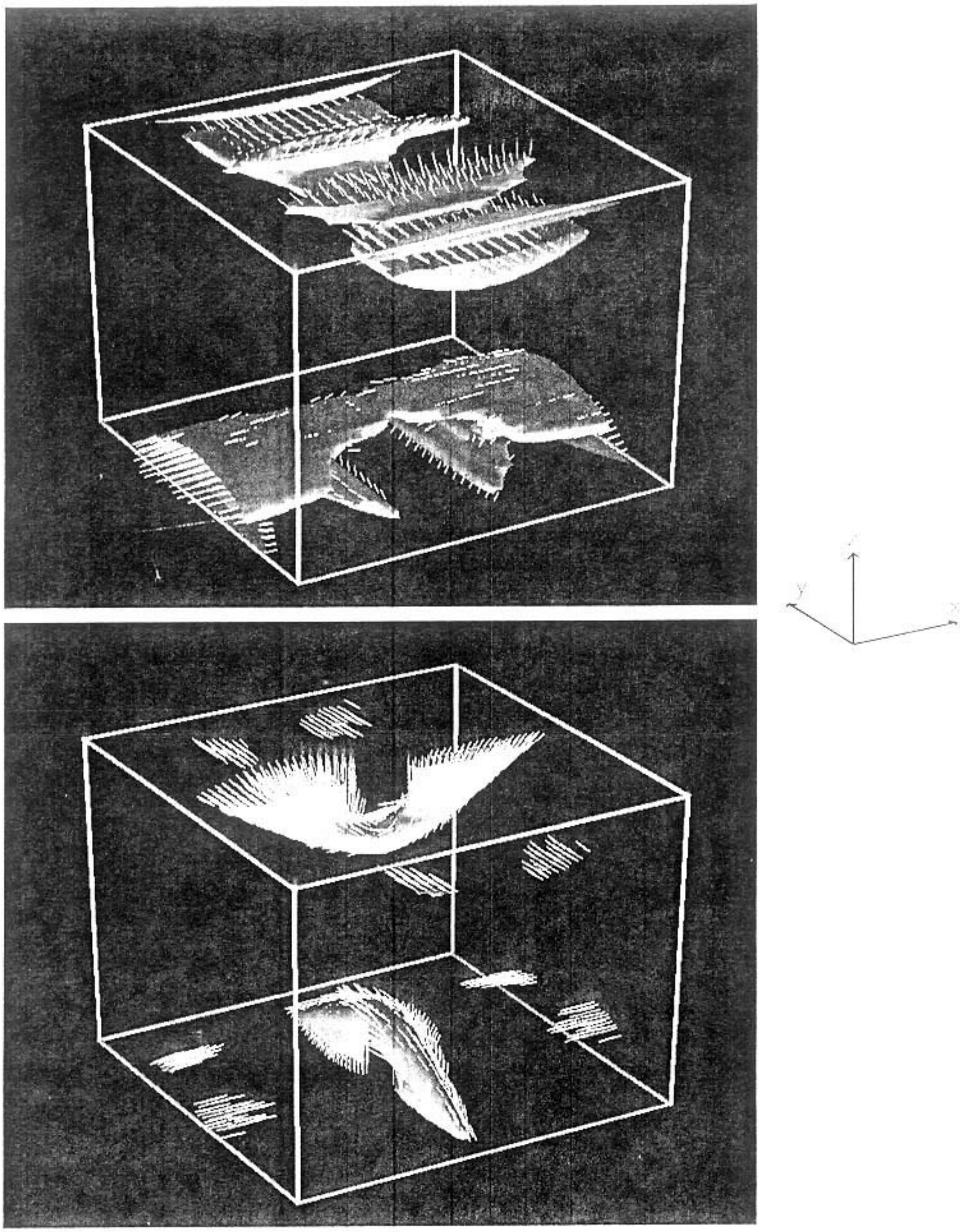

Figure 5. The magnetic configuration contains a double null-point. The orientation of the domains is indicated by the the small coordinate system to the right of the two panels. The images contain isosurfaces of current magnitude and current vectors above a minimum threshold. The top panel represents one-sided $m = 0$ mode perturbation of both null-points (No. 1 in Table I), driving current concentrations along the their spine axes. The bottom panel shows the $m = 1$ structure with current accumulation in the null-points separator plane. The magnetic field is perturbed by driving with the systematic velocity profile on both the top and the bottom boundary simultaneously (No. 3 in Table I).

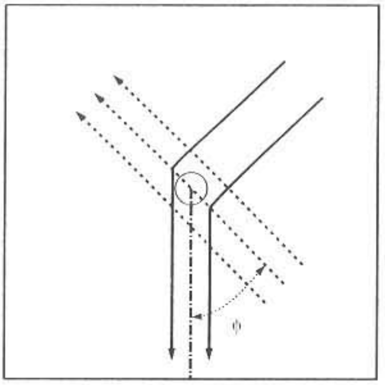

Figure 6. $m = 1$ mode perturbation of the spine axis of a double null-point. The plane indicates the fan plane with the circle indicating the position of the null-point and the dot-dashed line, the separator line. The dotted lines with arrows represent the velocity field perturbing the spine axis, having a ϕ degree angle relative the direction of the separator line. The solid lines show the characteristic of the current profile, with the pronounced kink in its direction around the null-point.

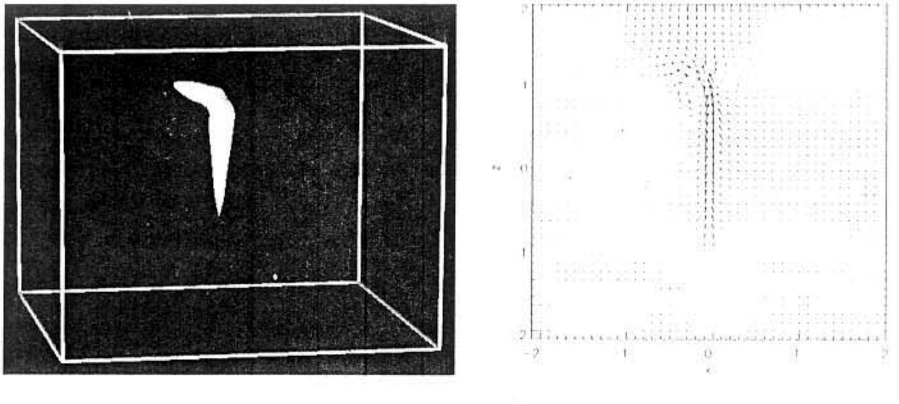

Figure 7. The left panel represents isosurfaces of constant current strength for No. 9 in Table II. The box is orientated with the x-axis to the right, the y-axis into the paper, and the z-axis up. The right panel shows current vectors in the plane of the strong current seen in the left panel. The spine axis of the top null passes through the front and back sides of the box.

with the separator line. Figure 7 contains both an isosurface image showing the bend in the current amplitude at the null-point and current vectors in the fan plane of the perturbed null. The driving velocity field in this case has an orientation of 45 deg to the separator line. Simultaneously it is seen that when only the region around one of the null-point spine axes is stressed, the second null-point acts as a boundary for the current along the separator.

An experiment was made where the non-perturbed null-point was removed from the domain by putting a z-boundary across the separator line. The current signature obtained in this case was similar to that seen for the same fraction of the full domain. This indicates that the topology defined by the multiple null-points is important for the temporal evolution, though the exclusion of a single null-point from the domain by introducing an artificial boundary has less importance, for this particular case.

4.1.2. *Force-Free Magnetic Field*

To look for dynamical differences between potential and force-free magnetic fields of similar topologically structure, the same experiments discussed in the previous section (Table I and Nos. 6–10 in Table II), were applied to the constant-α force-free magnetic field defined by Equation (7) having the spine axis of the top null aligned with the x-axis. To get a clear picture of the current structures arising from the perturbations, the zero-order current (the initial current) was subtracted from the actual current before analysing its structure.

This reveals that the force-free magnetic field reacts in a way that is consistent with the evolution found for the potential magnetic field. Both of the one-sided m modes (Table I) give almost identical signatures, with the most pronounced difference being the ratio of the current strength through the null-points to the current strength of the structures locally associated with the boundaries. This suggests that the magnetic fields different relation to the 'far away' field becomes important when truncated by arbitrarily applied boundaries. The fact that the potential field only contains the two null-points and the force-free magnetic field is a part of a fully 3D periodic magnetic field, makes the two fields dynamical response to the driving close to the boundaries strongly related to the exact location of the boundaries. As we are interested in the dynamics close to the null-points and their separator line, this discrepancy between the potential and the force-free field is of no importance for the conclusions of this investigation.

4.1.3. *Summary of m-Mode Perturbations*

When the m-mode experiments are performed on the z-boundaries, the resultant current structures resemble those found for an individual null-point exposed to the same type of perturbation. Only when the $m = 1$ mode is driven by perturbing the spine of one null in the pair is an important difference from the single null behaviour found. Namely that the separator acts as a strong accumulator of current, clearly distorting the orthogonal relationship between the orientation of the spine perturbation and the final current found in the single null experiments.

4.2. Shear perturbations

The m modes discussed above are only a small sample of the perturbation that are present in a realistic magnetic field; i.e., in the solar corona magnetic perturbations on both different time and length scales are found. This makes it sensible to expand the classes of perturbations that are investigated. In the solar photosphere both shear and compression flow topologies are observed and a natural extension would be to include such flows. Experiments with compression flows show only little impact on current distribution and the following sections concentrate on the shear experiments.

Several shear experiments are made on the surfaces parallel to the separator line (Nos. 1–5 of Table II). These include combinations of the shear wavelength and the number of domain sides that are used for stressing the magnetic field. The velocity profile used in these experiments is of the same type as shown in Equation (11), with the difference that the driving is on the x- and y-boundaries and that the domain for the three coordinate directions are in the interval $[-2, 2]$.

4.2.1. *Potential Magnetic Field*

It turns out that the experiment with driving on two domain sides, say the x-boundaries, provides a representative picture of the dynamic evolution in the double null-point system (No. 1 in Table II). This experiment is discussed in detail and only significant changes from this are mentioned for the other experiments.

In this experiment (No. 1 in Table II), the driving is confined to half of the z-domain $[-2, 0]$. This provides a shear across the spine axis of the null-point at (0,0,-1) and the part of the other null-points fan plane that connects to the boundary within this region. The field responds to the perturbation by driving two strong current patches along the separator. One part has a positive z-component along the separator (towards the null-point at $(0, 0, 1)$). A second part has a negative z-component along a small fraction of the separator, passing through the null-point at $(0, 0, -1)$, and extends all the way to the boundary at $z = -2$. By tracing magnetic field lines starting from the region around the point of current reversal on the separator, it is found that they connect to the boundary region where the driving velocity obtains its maximum value (the $(\pm 2, y, -1)$ lines). The explanation is found in the change of flow character that the driving field goes through at this location of space. The shear flow in the y direction is embedded in an envelope that makes the flow velocity go to zero at $z = \{-2, 0\}$. Then the flow, apart from being a shear flow, contains compression and decompression regions, and the division line becomes the trigger for the change in current direction along the separator. The magnetic field lines along a part of the zero velocity lines (the $(\pm 2, 0, [-2, 0])$ lines) of the shear profile are contained in the companion null-points fan plane and the distance between the field lines decreases as they approach the null-point. A wave is then naturally compressed in space, and the current associated with it has to increase. This provides a topological reason for accumulating current along the separator. As the current approaches the top null-point it spreads out over the fan plane close to the null and only an insignificant fraction of the current passes through the top null-point. Figure 8 illustrates the topologies discussed above. The vectors represent the driving profile at the boundaries. The red and yellow field lines show the magnetic field line topology around the null-points. The blue and green field lines indicate the difference in current connectivity along the separator.

When a similar perturbation is added to the y-boundaries, perturbing the spine axis of the null-point at $(0, 0, 1)$ (No. 2 in Table II), it can take one of two possible

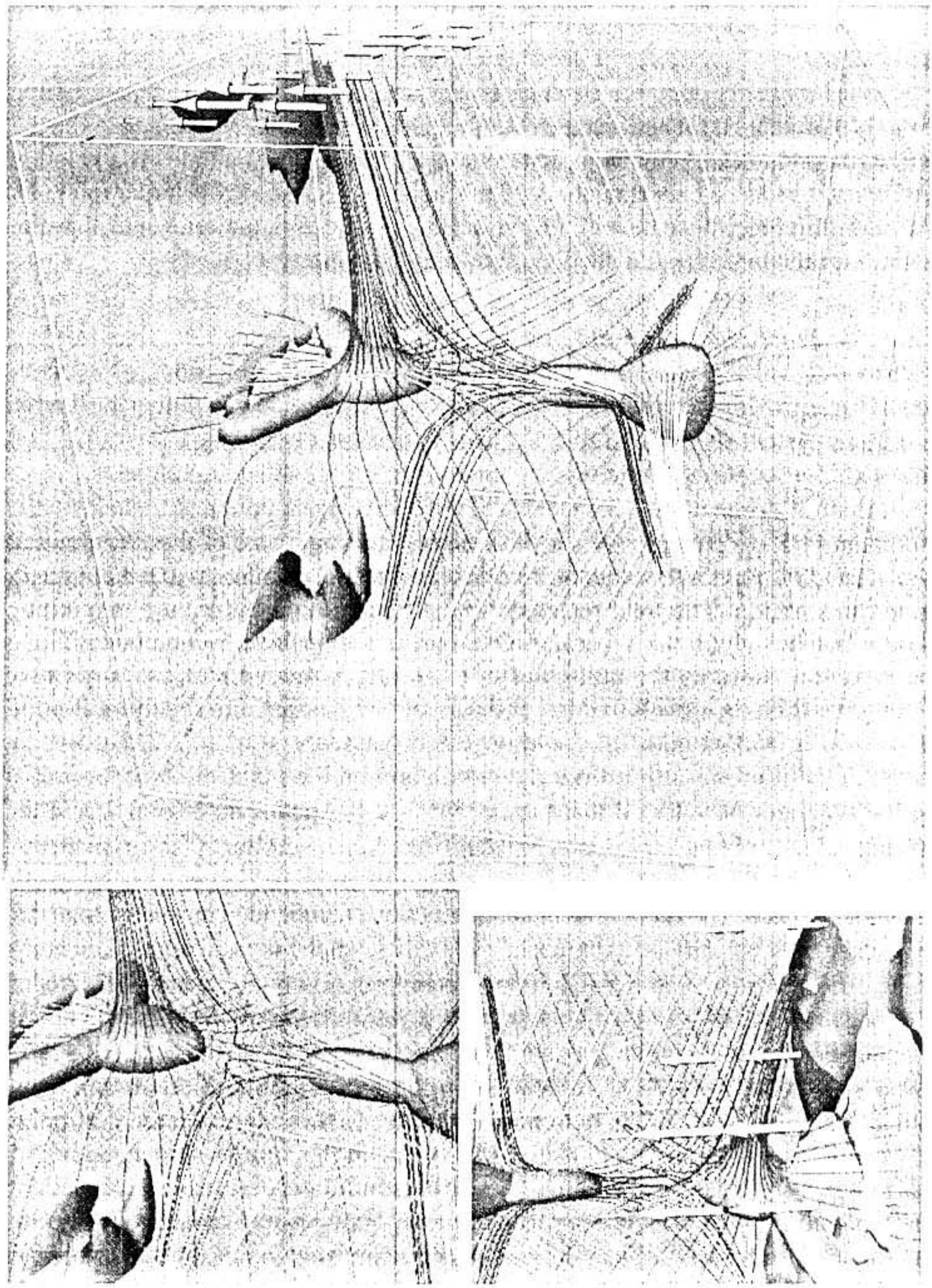

Figure 8. Yellow vectors indicate the driving pattern at the top boundary. The two reddish isosurfaces show the locations of the null-points and the lilac isosurfaces show the locations of strong current. Red and yellow field lines show the magnetic topology of the two nulls and the blue and green field lines provide the current topology. The blue current lines start from the strong current isosurfaces close to the right null-point (yellow field lines) and the green from the isosurface of the left null-point (red field lines). The top panel has the x-axis up, the y-axis out of the paper, and the z axis to the right. The same is the case for the lower left panel while the lower right is rotated 180 degrees around the x-axis and has the z-axis to the left.

orientations of the driving with respect profile on the x-boundaries. One can choose that the velocity profile has a continues first order derivative when passing the corners (an anti-symmetric profile with respect to the corners), or has a discontinues first derivative (a symmetric profile). This does not provide a problem in this experiment as the driving on the two boundaries are confined to each their half part of the z-domain. The current topology around the null-point at $(0, 0, -1)$ remains the same for both cases of driving, and a similar current structure arises at the other null-point. For the 'anti-symmetric' driving the number of current structures along the separator line increases to three. The current through the two null-points has the same direction and the current in the middle has the opposite direction. When imposing the 'symmetric' driving profile, the current direction of the top null-point reverses and the third component almost vanishes. This behaviour of the current patterns can be understood in terms of adding current contributions as seen from the previous experiment (No. 1 in Table II) onto the two null-point locations. It is therefore clear that the relative strength of the three components depends on both the amplitude and the orientation of the driving velocities on the two sets of boundaries.

Two more experiments were conducted. In these the driving was extended to include the full height in the z-direction. The difference between experiment Nos. 1 and 3 in Table II is the change of location for the reversal of current. It is moved closer to the top null-point, and it is an effect that would be expected from the change in the driving profile (the localisation of the compression/decompression line has changed).

When shear driving is applied on all four boundaries (No. 4 in Table II), it generates an uni-directional current along the separator, through both null-points and all the way to the z-boundaries. This current is due to the two contributions arising from driving on each of the two sets of boundaries ('anti-symmetric' around domain boundaries). The result is a current accumulation along the separator that is almost uniform in strength and stronger than the current that arises when only one set of boundaries is perturbed. As the current passes through the null-points it spreads out over a larger part of the fan planes, resulting in a significant drop in current magnitude. This four-sided shear driving provides the strongest current accumulation on the separator line and is the only experiment with an one directional current pattern all the way along the separator.

4.2.2. *Force-Free Magnetic Field*

Two sets of shear experiments are made with the force-free magnetic field defined in Equation (7). After changing the coordinate system, two magnetic null-points are located at $(0, 0, \pm\sqrt{2})$. In one case, the spine axes are along $(\sqrt{\frac{2}{3}}, \pm\sqrt{\frac{1}{3}}, 0)$ and for the second case, the spine axis of the null at $z = \sqrt{2}$ is aligned with the x-axis and the second is along $(\frac{1}{3}, \frac{\sqrt{8}}{3}, 0)$.

The difference between the two orientations is the way that the fan plans map onto the domain boundaries. In the force-free magnetic field the null-point spine axes are not orthogonal, as for the potential magnetic field, and the fan plane of one null-point has to twist around the separator line as it approaches the other null-point spine axis. How this divides the boundaries into regions of independent magnetic connectivity depends on the null-point orientation in the numerical domain and it makes predictions of the effect from boundary driving more complicated.

For the first orientation of the magnetic field (spine axes along $(\sqrt{\frac{2}{3}}, \pm\sqrt{\frac{1}{3}}, 0)$), three magnetically independent domains are perturbed from driving on only one of the x- or y-boundaries. As the null-point spine axes are not orthogonal in an $x-y$-projection, the divisions of the x- and y-boundaries, with regard to topological distinct regions, are located at significantly different locations. The applied shear driving (Nos. 3 and 4 in Table II) therefore provides different perturbations of the field on either side of the fan plane that penetrates the boundary on which the perturbation is applied.

Driving on the x-boundaries (No. 3 in Table II) mainly one domain is affected and the applied shear mostly goes into changing the field-line tension in this domain. The current arising from this perturbation aligns along the separator line, through the null points and towards the z-boundaries. As most of the field lines getting close to the separator line are in fact tied to the same boundary at two locations, the choice of shear direction naturally affects the change in distance (stretching/compressing) between the foot points of a given field line. It is found that the driving that stretches the field lines between the null-points builds up a current strength along the separator that is on the order of three times larger than for the case where the field is being compressed by the flow.

When the y-boundaries are perturbed (No. 4 in Table II) a much weaker current arises at the separator, clearly weaker in strength than the current patterns that are related to regions close to the boundary. In this case the penetrating fan plane is found, for a large part of the distance between the two null-points, to lie in an unidirectional flow. The field lines on either side of the fan plane are then exposed to almost the same perturbation, and a general shear across the fan plane is only a small one. As it is only field lines close the the fan plane that can get close to the separator, this type of perturbation is never found to produce significant current accumulations along the separator line.

For the second setup, where the spine axis at the upper null-point is aligned with the x axis, the picture changes from what was just described. Three experiments were made to compare the response to the one seen for the potential magnetic field (Nos. 1–5 in Table II) that was discussed in the previous section. They represent shearing over the full z-height, and provide driving on either the x, the y, or all four boundaries simultaneously (Nos. 3–5 in Table II).

When driving on the x-boundaries (No. 3 in Table II), the strongest current appears at the top null-point (the spine axis penetrates the driving boundary). The

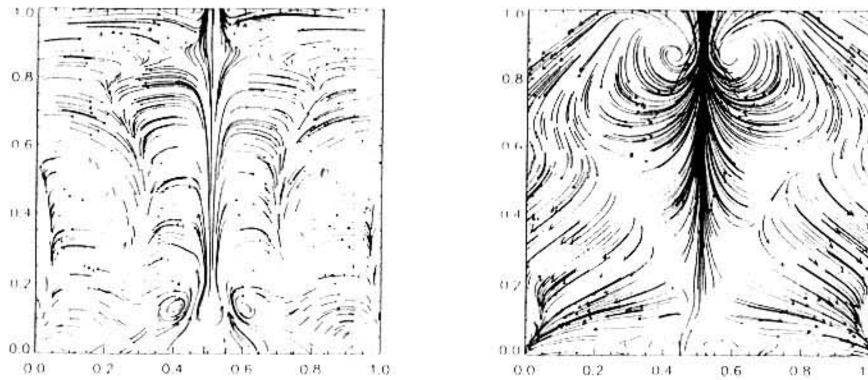

Figure 9. Force-free magnetic field configuration with the top null-point spine axis aligned along the x-direction. Trace lines of current in the null-points fan plan. The left panel represents the fan plane of the top null-point ($y - z$-plane), and the right panel is approximately the fan plane of the lower null-point ($x - z$-plane). The field is stressed by a shear flow over the full z-length on both x-boundaries (No. 3 in Table II).

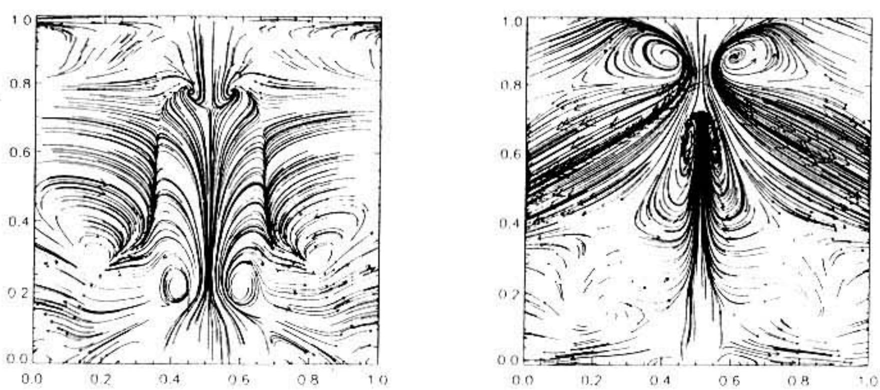

Figure 10. Panels as in Figure 9. The shear flow is here on the y-boundaries (No. 4 in Table II).

current structure in both fan planes has a double vortex structure, with the current at the nulls being along the separator, though the current through the null at $z = -\sqrt{2}$ is much weaker than at the other null. The current direction is the same at both nulls and is found to continue all the way along the separator. This is different from the results found for the potential experiments, where this type of driving exhibits two different current directions along the separator. Figure 9 shows field-line traces of the current in the fan planes of the two null points.

When driving is applied on the y-boundary (No. 4 in Table II), the current again shows the double vortex structure at the nulls. This time the current through the nulls has different orientations. The strongest current is associated with the bottom null-point, and this current orientation dominates along most of the separator, Figure 10.

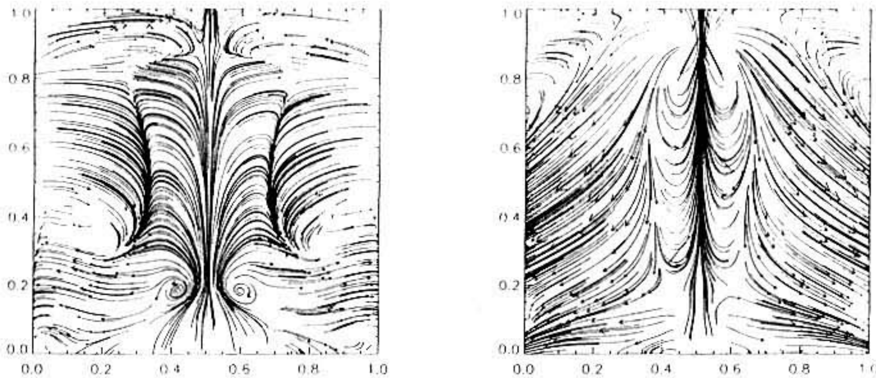

Figure 11. Panels as in Figure 9. The shear flow is applied on both the x- and the y-boundaries (No. 5 in Table II).

When the two perturbations are combined in one experiment, the lower null-point shows a clear double vortex current structure in its fan plane, while the top null-point has a much less clear signature. The current is one directional along the separator, and extends all the way to the z-boundaries. Just one grid point away from the separator, the current is either converging towards (in the $y-z$-plane) or diverging away from (in the $x-z$-plane) the separator, Figure 11. In the overall picture it is found that the current magnitude is strongest at the bottom null-point, where the large double vortex current structure is located.

4.2.3. *Summary of Shear Perturbations*

The potential and force-free experiments show the same characteristics in their respond to the shear perturbation, the double vortex structure of the current centred on the null-points, and a general current accumulation along the separator. There are differences between the two magnetic fields in their responses to the same driving: some of these are related to the difference in the orientation of the null-points relative to the driving boundaries, and others to the field topology at the boundaries. Probably the most significant difference is the tendency for the force-free magnetic field to host an unidirectional current all along the separator, instead of creating current patches with different orientations along the separator, as was generally found for the potential experiments. The experiments show that it is of vital importance to know the orientation of the driving relative to the null-point pair's topological structure. Only with the combined knowledge of the magnetic field type and the orientation of the perturbation may it be possible to determine the current flow that will be generated in a double null-point configuration.

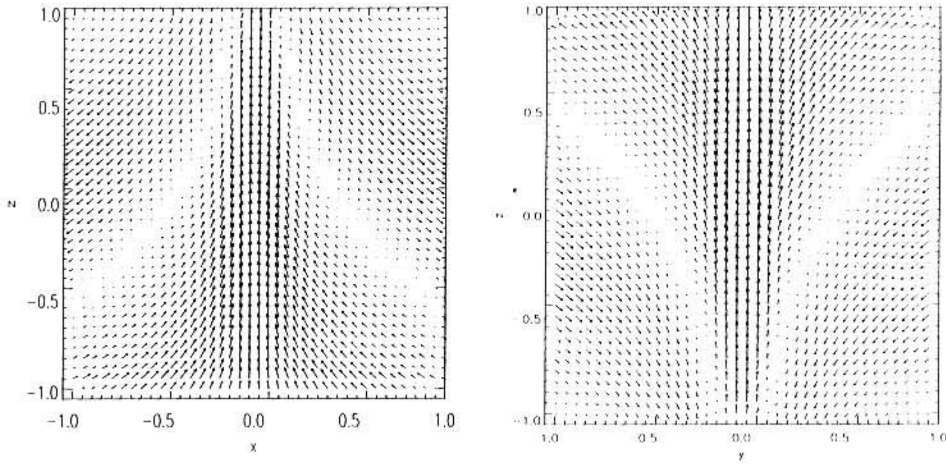

Figure 12. The domain only includes a part of the separator defined by the two nulls in the potential magnetic field (Equation (6)). The field is perturbed by systematic shear motions on both the x- and y-boundaries over the full length of the domain (No. 5 in Table II). Vector plots of the current components in two planes through the separator. The left panel shows the $x - z$-projection and the right panel the $y - z$-projection.

5. Separator Lines

It was pointed out by Démoulin, Hénoux, and Mandrini (1994) that flaring in some cases occurred in connection with parts of separator lines, but not necessarily in the vicinity of nulls. It is therefore of interest to investigate the dynamical behaviour of a part of a separator line. This is done by taking the potential magnetic field and truncating the domain to contain only the central part of the separator line defined by the two nulls. Despite the fact that the field does not contain a real separator line after the truncation, the same name will be used to identify the truncated part of the real separator line. This field is then exposed to the shear perturbations that were found to generate strong current accumulation along the separator line in the potential double null-point experiments discussed above (No. 5 in Table II).

A restriction in the evolution of the field lines in the domain is imposed by the applied line tying on the boundaries. On the driving boundaries this provides the means for stressing the field, while on the boundaries without driving (zero velocity) it fixes the end points of the field lines and to some extent limits the free evolution of the field. In the experiments having magnetic singularities located in the domain it is found that this condition does not limit the possibility for developing 'singularities' in the current distribution. One could therefore expect that, even for a field without magnetic singularities, singularities can develop if the dynamics of the field allows any to form.

Above it was found that shear velocities along the separator line gave rise to different current profiles along this line. When the same driving profiles are applied to the truncated field, the current does not concentrate along the separator in a singular manner, but maintains a finite structural resolution, as seen in Figure 12. These experiments show that the complexity of the current topology depends on the wavelength of the applied boundary driving. When the shear profile on the $x-y$-boundaries involves the full domain in the z-direction (No. 5 in Table II), then the current flow in the vicinity of the separator line is concentrated in two orthogonal plane regions. If the two planes were extended out of the domain, one end would hit one null-point and the other end would stretch out along the spine axis of the other null-point. These surfaces are orthogonal and the current is seen to change partly between them as the current flows from one end of the domain to the other. Outside this region the current flows in the opposite direction and the domain contains two differently orientated current structures, Figure 12. When the wavelength of the systematic shear pattern is reduced in the z-direction (i.e., more that one shear pattern along the z-direction) the number of current reversal layers in a, say the $x-z$, plane through the separator increases. But it does not change the topology of the current along the separator line in the domain. By comparing the current amplitude in the shells of different orientation, it is found that they all are of the same order of magnitude. By comparing the current structure in these experiments with the experiments that included the null-points, it is seen that the developing current structures are a consequence of the null-points that define the field topology. The important difference between the domains with and without the nulls is that only the field containing null-points is able to provide a current structure that collapses along the separator line, while, probably, the change in topology prevents the current from collapsing in the isolated separator experiments. It is then of natural interest to investigate how different boundary conditions, on the non-driven boundaries, influence the non-collapsing result. From the present investigation it is not possible to derive a full conclusion of whether isolated separator lines are likely to collapse or not under other boundary conditions.

6. Conclusion

An investigation of the current topology has been undertaken in relation to magnetic field-line topologies that contain separator lines. A separator line is defined by the intersection of two separatrix surfaces. The existence of separatrix surfaces requires the presence of some form of zero in the magnetic field where it is not in a trivial structure. The full 3D version of such is the 3D null-point, with objects like null lines or surfaces being structurally unstable to perturbations. It is expected that for a real and stable separator to exist, there have to be two magnetic null-points that are physically connected by the separator, as in the magnetic fields defined in Equation (6) and Equation (7). In magnetic fields where null-points do not exist, there can exist local field lines where the topology is similar to that of a separator, an x-type topology in the plane orthogonal to the magnetic field direction. Such lines are called quasi-separatrix lines and may account for dynamical events that can trigger magnetic reconnection (Priest and Démoulin, 1995). Different methods may be used to identify null-points (Lau, 1993; Démoulin *et al.*, 1994) in complex models, it may be vital to resolve the magnetic field almost down to the linear domain of the null-point. When this is not the case, one can draw the wrong conclusion, namely that null-points are not present within the field topology. In this paper we have limited our aim to investigate the influence of real separator lines, and leave a discussion of quasi-separator lines for a later paper.

The main results from the numerical experiments are:

– Both spine and fan reconnection modes can be excited in double null-point systems. The fan reconnection mode is the easiest to excite and probably the only one interesting for nulls in real magnetic fields. Further,

– a separator line indeed appears to act as an attractor for singular current accumulation IF both nulls are present in the numerical domain. Hence,

– when the nulls are excluded from the domain, the remains of the separator do not appear to produce such an accumulation.

– The presence of nulls would therefore seem paramount if topological current accumulation is to occur.

The experiments have shown that the double null-point topology is important in determining the locations where current accumulates in magnetic fields. The investigation confirms that it is possible to drive current through the null-points, both in the fan plane and along the spine axes, when the right perturbations of the field topology are made. Additionally it is found that the separator becomes an important location for current accumulations for several driving combinations. The current topology depends strongly on the topology of the applied driver and its orientation relative to the fan planes and spine axes of the two null points. The m modes found by the linear analysis of the single axisymmetric null (Rickard and Titov, 1996) are found to exist in a modified form for the null-point pair, with a current signature that is clearly altered by the nonlinearity of the magnetic field topology for the vast majority of the possible ways of driving it. This is most clearly seen in the case where the mode is perturbed by tilting the spine axis of a null-point. To drive a strong singular current along the separator line of the null-point pair, using a shear perturbation along the separator, the wavelength of the perturbation has to be more than twice the separation between the null-points. When this is not fulfilled several current structures may arise along the separator line, providing the possibility for more localised reconnection to occur. In these events the energy released has to be limited, as only a small group of magnetic field lines can be expected to interact in such an event. We expect that the most reconnective mode of the double null-point pair, is the one where current accumulates all along the full length of the separator line, just as seen in the experiment of Galsgaard and Nordlund (1997).

The difference between the potential, Equation (6), and the force-free, Equation (7), magnetic field response to the applied perturbations seems to be minor. Most of the observed differences are found to relate to structural difference in the magnetic field close to the imposed boundaries, and this is of little importance for the structural evolution close to the null-points and the separator. An important difference is the tendency for the force-free field to provide an unidirectional current along the separator with a higher likelihood than the potential field. It therefore seems more likely to drive separator reconnection all along the separator in force-free magnetic fields than in potential magnetic fields. This could be an artifact of the chosen force-free magnetic field and should be tested with other descriptions of force-free double null-point magnetic fields. Before this is finally settled there are reasons to compare results from both potential and force-free extrapolations of magnetic field topologies.

The experiments with only the separator line included in the numerical domain show a significant difference from the similar experiments containing null-points. In these experiments it was not possible for the current to collapse along the separator line. This shows that the null-points defining the separator are important, and that the isolated separator, with the applied boundary conditions, has no significant influence on the current accumulation, as it is not collapsing along it. This raises an important question, what influence does the frozen-in condition on the boundaries have on this result? It was found that this restriction did not influence the fields capability to collapse along the separator while the nulls were included, it would therefore not be expected to be an obstacle for the current to collapse when they are excluded IF the dynamical evolution of the field would allow it.

An important question regarding the magnetic field topologies is the existence of 3D magnetic null-points. Present investigations of the solar magnetic field are based on either potential or force free model extrapolations of the observed flux distribution at the photosphere. These are difficult to do and time consuming to investigate for magnetic null points and locations of separatrix surfaces and separator lines. The present results show that only in a few cases are null points found above the photosphere, and they seem not to be involved in the energy release related to the observed Hα emission from flares. The modelling is limited in its complexity as a consequence of the limited resolution of magnetograms and the assumption of potential or force-free magnetic fields being representative for the coronal field. Strong (1993) finds that many 'non-active' regions in the corona show constant dynamical changes, which is also seen on *Yohkoh* and SOHO movies of the Sun. This is inconsistent with the assumption that the coronal field is in an almost force-free state. If these facts are combined in the right way, they may favour the existence of many singularities in the corona on length scales that our present models/observations are not able to show.

Acknowledgements

R.V.R. is grateful to PPARC for financial support for a 2 month visit to St. Andrews. K.G. and G.J.R. thank PPARC for financially supporting their positions. The authors acknowledge Pascal Démoulin's helpful advice for improving the presentation of the paper.

References

Craig, I. J. D. and Fabling, R. B.: 1996, *Astrophys. J.* **462**, 969.

Craig, I. J. D., Fabling, R. B., Henton, S. M., and Rickard, G. J.: 1995, *Astrophys. J.* **455**, L197.

Craig, I. J. D. and Henton, S. M.: 1995, *Astrophys. J.* **450**, 280.

Dahlburg, R. B., Antinochos, S. K., and Norton, D.: 1996, *Phys. Rev. E*, submitted.

Démoulin, P., Hénoux, J. C., and Mandrini, C. H.: 1994, *Astron. Astrophys.* **285**, 1023.

Démoulin, P., Mandrini, C. H., Rovira, M. G., Hénoux, J. C., and Machado, M. E.: 1994, *Solar Phys.* **150**, 221.

Fukao, S., Masayuki, U., and Takao, T.: 1975, *Rep. Ionos. Res. Japan* **29**, 1120.

Galsgaard, K.: 1991, 'Topology of Magnetic Fields in Three Dimensions', Master thesis, The University of Copenhagen.

Galsgaard, K. and Nordlund, Å: 1996a, *Astrophys. Letters Comm.* **34**, 175.

Galsgaard, K. and Nordlund, Å: 1996b, *J. Geophys. Res.* **101**, 13445.

Galsgaard, K. and Nordlund, Å: 1997, *J. Geophys. Res.* **102**, 231.

Green, J. M.: 1989, *J. Geophys. Res.* **93**, 8583.

Hesse, H. and Schindler, K.: 1988, *J. Geophys. Res.* **93**, 5559.

Lau, Y.: 1993, *Solar Phys.* **148**, 301.

Lau, Y. T. and Finn, J. M.: 1990, *Astrophys. J.* **350**, 672.

Otto, A.: 1995, *J. Geophys. Res.* **100**, 11863.

Parnell, C. E., Smith, J. M., Neukirch, T., and Priest, E. R.: 1996, *Physics Plasma* **3**, 759.

Priest, E. R. and Démoulin, P.: 1995, *J. Geophys. Res.* **100**, 23443.

Priest, E. R. and Titov, V. S.: 1996, *Phil. Trans Roy. Soc. London* **A354**, 2951.

Reddy, R. V., Watanabe, K., Watanabe, T., and Sato, T.: 1995, *J. Phys. Soc. Japan* **64**, 124.

Rickard, G. J. and Titov, V. S.: 1996, *Astrophys. J.* **472**, 840.

Strauss, H. R.: 1991, *Astrophys. J.* **381**, 508.

Strong, K. T.: 1993, in S. Enome and T. Hirayama (eds), 'New Look at the Sun with Emphasis on Advanced Observations of Coronal Dynamics and Flares', *Radioheliographs Series* No. 6., p. 53.

Syrovatskii, S. I.: 1981, *Ann. Astron. Soc. Astrophys.* **19**, 163.

Watanabe, K. and Sato, T.: 1990, *J. Geophys. Res.* **95**, 75.